NeuroImage 274 (2023) 120128

Contents lists available at ScienceDirect

NeuroImage

journal homepage: www.elsevier.com/locate/neuroimage

Coherent, time-shifted patterns of microstructural plasticity during motor-skill learning

Michela Azzarito[a,1], Tim M. Emmenegger[a,1], Gabriel Ziegler[b,c], Eveline Huber[a], Patrick Grabher[a], Martina F. Callaghan[d], Alan Thompson[e], Karl Friston[d], Nikolaus Weiskopf[f,g], Tim Killeen[a], Patrick Freund[a,d,f,*]

[a] Spinal Injury Center, University Hospital Balgrist, University of Zurich, Zurich, Switzerland
[b] Institute of Cognitive Neurology and Dementia Research, Otto-von-Guericke-University Magdeburg, Magdeburg, Germany
[c] German Center for Neurodegenerative Diseases (DZNE), Magdeburg, Germany
[d] Wellcome Centre for Human Neuroimaging, UCL Queen Square Institute of Neurology, University College London, London, United Kingdom
[e] Department of Neuroinflammation, UCL Institute of Neurology, University College London, London, United Kingdom
[f] Department of Neurophysics, Max Planck Institute for Human Cognitive and Brain Sciences, Leipzig, Germany
[g] Felix Bloch Institute for Solid State Physics, Faculty of Physics and Earth Sciences, Leipzig University, Leipzig, Germany

ARTICLE INFO

Keywords:
Myelin plasticity
Multiparametric mapping
Magnetisation transfer
Motor learning
Quantitative MRI
Corticospinal tract
Hippocampus

ABSTRACT

Motor skill learning relies on neural plasticity in the motor and limbic systems. However, the spatial and temporal characteristics of these changes—and their microstructural underpinnings—remain unclear. Eighteen healthy males received 1 h of training in a computer-based motion game, 4 times a week, for 4 consecutive weeks, while 14 untrained participants underwent scanning only. Performance improvements were observed in all trained participants. Serial myelin- and iron-sensitive multiparametric mapping at 3T during this period of intensive motor skill acquisition revealed temporally and spatially distributed, performance-related microstructural changes in the grey and white matter across a corticospinal-cerebellar-hippocampal circuit. Analysis of the trajectory of these transient changes suggested time-shifted cascades of plasticity from the dominant sensorimotor system to the contralateral hippocampus. In the cranial corticospinal tracts, changes in myelin-sensitive metrics during training in the posterior limb of the internal capsule were of greater magnitude in those who trained their upper limbs vs. lower limb trainees. Motor skill learning is associated with waves of grey and white matter plasticity, across a broad sensorimotor network.

1. Introduction

Motor skill learning of a complex sensorimotor task, such as juggling or dancing, requires physical and cognitive effort and relies on functional changes and interactions between and within cortical and subcortical brain areas (Boyke et al., 2008; Dayan and Cohen, 2011; Draganski and May 2008; Hüfner et al., 2011; Jacobacci et al., 2020; Scholz et al., 2009; Taubert et al., 2016). Studies using magnetic resonance (MR) imaging have demonstrated grey (GM) and white matter (WM) changes accompanying the acquisition of specific skills in brain regions engaged by the task or activity (Draganski and May 2008; Zatorre et al., 2012). Volumetric GM changes have been observed in the hippocampus after acquiring expertise in dancing (Hüfner et al., 2011) and spatial navigation tasks (Maguire et al., 2000), and in the putamen of skilled pianists (Granert et al., 2011). Even when skills are acquired by non-experts over much shorter timescales, ranging from hours to days, GM changes are apparent in the sensorimotor cortex (M1), for instance after balance training (Taubert et al., 2016). Such adaptive changes in M1 during motor learning have been associated with shifting interactions within and across subcortical areas, includ-

Abbreviations: CSF, cerebrospinal fluid; %CSR, percent correct stimulus responses; CST, cranial corticospinal tract; EC, hippocampus-entorhinal cortex; FWE, family wise error; FoV, field of view; FWHM, full-width at half-maximum; GM, grey matter; GRAPPA, generalised autocalibrating partially parallel acquisitions; GCUT, graph-cut/region-growing; M1, sensorimotor cortex; MR, magnetic resonance; MT_{sat}, magnetisation transfer saturation; MPM, multi-parameter mapping; MNI, Montreal Neurological Institute; PD, proton density; R1, longitudinal relaxation rate; R2*, transverse relaxation rate; RT, response time; RF, radio-frequency; SPM, statistical parametric mapping; TE, echo times; TIV, total intracranial volume; VBM, voxel-based morphometry; WM, white matter.

* Corresponding author at: Spinal Cord Injury Center, University Hospital Balgrist, Forchstrasse 340, 8008 Zurich, Switzerland.
[1] Contributed equally.
E-mail address: patrick.freund@balgrist.ch (P. Freund).

https://doi.org/10.1016/j.neuroimage.2023.120128.
Received 19 August 2022; Received in revised form 14 April 2023; Accepted 17 April 2023
Available online 26 April 2023.
1053-8119/Crown Copyright © 2023 Published by Elsevier Inc. This is an open access article under the CC BY license (http://creativecommons.org/licenses/by/4.0/)

ing the cerebellum, thalamus and the hippocampus (Blakemore et al., 1999; Doyon and Benali, 2005; Jacobacci et al., 2020; Middleton and Strick, 2000; Sakayori et al., 2019; Sehm et al., 2014; Sommer, 2003; Watson et al., 2019). The trajectory of these changes suggests that the biological substrate of learning follows a sequence of expansion, selection, and renormalisation, although the precise nature of these processes remains unresolved (Boyke et al., 2008; Draganski et al., 2006; Fu and Zuo, 2011; Makino et al., 2016; Scholz et al., 2009; Weber et al., 2019; Wenger et al., 2016).

GM and WM changes in MR neuroimaging have been associated with visual, somatosensory and motor cortical neuroplasticity, performance improvement, oligodendrogenesis and myelination in mice (Badea et al., 2019; Gibson et al., 2014; Lamprecht and LeDoux, 2004; Theodosis et al., 2008). More recently, MR techniques using computational modelling of quantitative multi-parameter mapping (MPM) have been developed (Dick et al., 2012; Freund et al., 2019; Leutritz et al., 2020), allowing inferences of quantitative microstructure, including myelin, by means of the longitudinal relaxation rate (R1=1/T1) (Dick et al., 2012; Natu et al., 2019; Weiskopf et al., 2021), magnetisation transfer saturation (MT_{sat}) (Georgiadis et al., 2021; Helms et al., 2010, 2008; Weiskopf et al., 2021), and iron via the effective transverse relaxation rate (R2*) (Langkammer et al., 2010; Natu et al., 2019; Weiskopf et al., 2021). These modalities have been used to demonstrate changes indicating demyelination in the CNS of humans following spinal cord injury (David et al., 2019; Freund et al., 2019).

Hitherto, motor tasks used to explore training effects have had limited applicability in rehabilitation, with unicycling and juggling of little relevance to most patients with significant neurological injury or disease, such as spinal or brain injuries, stroke or multiple sclerosis. We aimed to study the evolution of GM and WM volume changes—uniquely adding longitudinal MPM analyses—in the brains of healthy individuals during 1 month of intensive sensorimotor training in a task that is challenging, yet feasible, for neurological patients and healthy individuals alike, and which is applicable to both the upper and/or lower limbs (Prahm et al., 2017). Participants learned to perform increasingly complex and rapid sequences of movements of either their upper or lower limbs in response to visual and auditory cues. Using serial MR imaging before, during and after training, we aimed to characterise (i) the spatial and temporal evolution of training-induced changes across and within subcortical and cortical areas implicated in motor skill learning, (ii) the somatotopic changes specific to upper or lower limb training, and (iii) associations between structural changes and performance improvements.

The ecological training task selected for use in this study is based on an open-source dance and rhythm game used for recreation and rehabilitation, known for its modifiability, variable difficulty and for its capacity to provide a challenging, fun and motivating game experience (Höysniemi, 2006; Prahm et al., 2017). Playing is known to recruit key attentional, integrative and sensorimotor brain networks (Eggenberger et al., 2016; Noah et al., 2015) and is expected to engage hippocampal circuits involved in the consolidation of motor sequence learning (Albouy et al., 2008; Long et al., 2018), with the combination of multi-joint physical activity and cognitive and sensorimotor stimulation (Kempermann et al., 2010; Rehfeld et al.,2017). While activation of some neural elements will be common, irrespective of the limb trained, we anticipated differences between those training with the upper and lower limbs in regions with well-established somatotopy, including the sensorimotor and corticospinal systems. Specifically, we anticipated that transient or enduring myelin increases would be reflected in MT_{sat} values and that iron would be locally consumed (Carlson et al., 2007; Tran et al., 2015), and reflected in R2* values. Furthermore, both values could return towards baseline during the subsequent consolidation / pruning phase.

Recruitment to this study was restricted to males in light of the preponderance of males affected by (incomplete) traumatic spinal cord injury, which is the primary target of the training intervention investigated here. A secondary consideration was limited fMRI evidence that cortical and subcortical activations during motor learning evince systematic sex differences (Lissek et al., 2007). The feasibility of transferring this training intervention to patients with spinal cord injuries has been demonstrated in a pilot study (Villiger et al., 2015).

2. Materials and methods

2.1. Participants

In this exploratory, longitudinal training study, thirty-two healthy, right-handed adult males (age range: 23–62 years; supplementary material 1) were recruited and split into three training groups (upper limb training [$n = 9$]; lower limb training [$n = 9$]; no training [$n = 14$]). All had normal or corrected-to-normal vision, no history of psychological or neurological disease, and no contraindications to MRI. All participants were naive to the experimental setup. The first six participants were block randomised to either upper, lower or no training groups, after which an age-matching algorithm was used to ensure comparability with our typical spinal cord injury patients (young to middle-aged males (Jackson et al., 2004)) for future studies including patient cohorts.

2.2. Standard protocol approvals, registrations, and patient consents

The study was carried out in accordance with Good Clinical Practice and the Declaration of Helsinki and approved by the Zurich cantonal ethics committee (KEK-2013–0559). All participants gave written, informed consent.

2.3. Training task

Participants undertook training over 4 consecutive weeks (60 min training, 4x per week, Fig. 1A). They were not allowed to train on the task between day 28 and day 84, when an assessment of performance retention was made. Upper and lower limb training utilised StepMania 5 Beta 3 (www.stepmania.com) for Windows 7 (Microsoft, La Jolla, CA) and an input device dependant on which limbs were to be trained (see below). During the game, arrows matching symbols on the input device (← ↑ → ↓) scrolled up the screen while a popular song played from the speakers. The participant was tasked with selecting and activating the correct symbol at the precise moment the scrolling arrow overlapped with a set of static arrows at the top of the screen with the moment of overlap synchronised to the beat of the music using the Dancing Monkeys script (Karl O'Keeffe, https://monket.net/dancing-monkeys/). The script generates patterns of arrows of varying difficulty but excludes sequences that would be impossible to respond to. Each bout lasted 120 s, after which the participant was given immediate visual feedback in the form of a percentage score (accurate response within 45ms: 2pts, 45–90ms: 1pt, >90ms: no score; cumulative score expressed as a percentage of maximum possible points). As the pattern of arrows differed for each bout, participants achieved improvement not by rote learning of a series of movements but by developing optimal strategies for adapting to the varying patterns (Orrell et al., 2006) – optimal response involved identifying and executing multi-step responses to frequently-encountered patterns of arrows as they were revealed. Each training session comprised 15 bouts, with approximately 120 s rest between each. Progress in the training involved moving through increasingly difficult levels whereby the number, pattern complexity and scroll speed of the arrows increased. The next level was unlocked when three non-consecutive scores of ≥ 80% were achieved within a level. Demotion to the previous level was mandated by three consecutive scores of ≤ 30%.

Participants allocated to the lower limb training group used a dance platform (Impact Dance Platform, Positive Gaming BV, Haarlem, Netherlands) as the input device and effectively learned to "dance" in response to the arrow stimuli (Fig. 1B, D). The platform was placed on

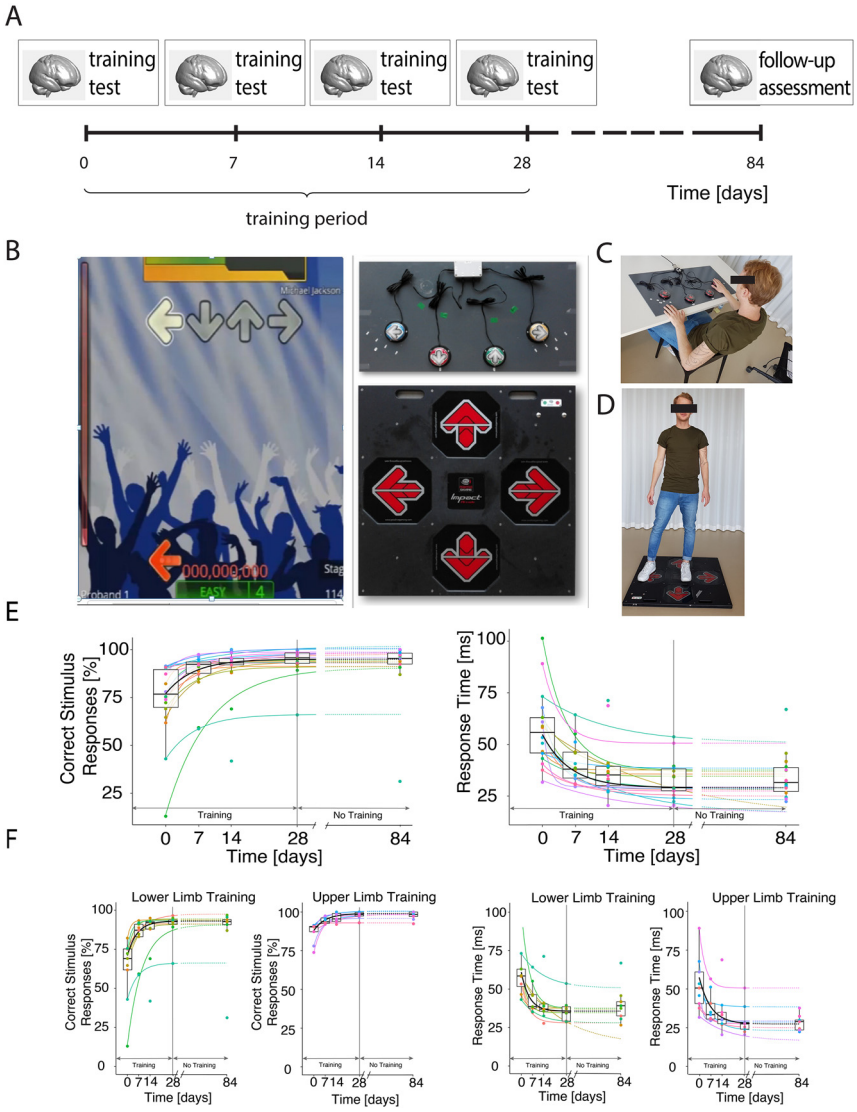

Fig. 1. Experimental design, training task and behavioural data (see accompanying video). The experimental design (A) included MRI acquisition and training assessments at baseline (day 0) during the training period (days 7, 14 and 28) and at final retention assessment (day 84). Sixty minutes of supervised training in a motor-skill task was undertaken four times per week for 4 consecutive weeks (B), whereby participants were required to activate inputs with their hands or feet (depending on whether they were allocated to the upper (C) or lower limb (D) training groups) in response to rhythmic aural and visual stimuli in the dance game Stepmania. The participant was tasked with selecting and activating the correct symbol at the precise moment the scrolling arrow overlapped with a set of static arrows at the top of the screen. Behavioural improvement, defined as the percentage of correct stimulus responses (%CSR), and response time (RT; the deviation in ms from the ideal response) were measured during a formal, standardised performance test at weekly intervals (see methods). Individual values for these metrics are plotted as coloured dots (E and F), while participant-specific behavioural curves were computed (coloured lines) along with the corresponding group mean (black line). The dashed lines connect the last training point (day 28) with the retention test on day 84. All participants demonstrated improvement in the task over time ($p<0.05$) and %CSR evolution was significantly different between the upper and lower limb trained groups, while this was not the case for RT.

the floor in a large, open space facing a TV monitor on which the game was displayed. Those allocated to the upper limb training group sat facing a table on which a custom-made platform, designed to be analogous to the lower limb platform, was placed (Fig. 1B, C). Participants were instructed to use their left hand for ← and ↑ and their right for → and ↓. A laptop was used to run the game.

Each participant progressed through the levels at different paces and were consistently challenged. To assess changes in task performance in a standardised manner, participants were assessed immediately prior to training (baseline) and again on days 7, 14, 28 of training and finally on day 84. These performance tests were conducted using a preprogrammed sequence of arrows including segments at 60, 80, 100 and 120 bpm and featuring patterns of increasing complexity for a total of 3 min 20 s set on a neutral, black background with the music replaced with a metronome. Importantly, the sequence of arrows presented differed for each test. Thus, each test was controlled in terms of overall difficulty but learning of the specific sequences was not possible. Cues (← ↑ → ↓) were balanced within and across segments to ensure no laterality effect. Response accuracy and response time data in these standardised performance tests were used as the basis for the behavioural analyses. Control participants undertook neither training nor the performance test and were instructed not to pursue new behavioural skills or take dancing classes during the study but to otherwise continue with their daily routines.

2.4. Behavioural analyses

Behavioural data were analysed using bespoke Matlab 2016b (The MathWorks, Natick, MA, USA) routines. Performance was measured as the percentage of correct stimulus responses (%CSR; defined as accurate inputs within 90 ms of a cue); and response time (RT), defined as the mean absolute delay in ms between cue overlap and correct inputs. These behavioural measurements were computed for each subject and each side (left/right). To evaluate the improvement of each subject, subject-specific model parameters were estimated as follows.

An exponential model of both behavioural parameters was computed over the training period using a nonlinear regression model:

$$y = \alpha - \delta e^{-\gamma t} + \varepsilon$$

where y is the training parameter (%CSR or RT); t is the training timepoint (baseline, day 7, 14 and 28), with random error Ɛ assumed to be normally distributed with a mean of 0. α is the 'asymptote', i.e. the value the training parameter eventually settles on over time (the plateau); δ is the 'acquisition climb', the extent of improvement from baseline to asymptote; and γ indicates the shape of the trajectory (i.e., how quickly it converges to asymptotic performance). These parameters were estimated for each participant by fitting the model to the subject's specific behavioural parameters. Parameters δ and γ were used to investigate: (i) skill acquisition in all participants; (ii) differences in training up-

per and lower limbs; (iii) left/right lateralised differences in training responses; and (iv) differences associated with MRI changes. The first three questions were assessed with Stata 15.0 (Stata Corp, College Station, TX); while the latter was assessed with SPM (Statistical Parametric Mapping version 12 v7487; https://www.fil.ion.ucl.ac.uk/spm). The distribution of performance metrics (in terms of δ and γ) was first assessed for normality using the Shapiro-Wilk test and analysed for all trained participants using one-sample Wilcoxon tests. To assess differences in performance when training the upper versus lower limb, a two-sample Wilcoxon test was performed on the γ and δ of all trained participants. Finally, to assess if the acquired skill was preserved at follow-up, a Wilcoxon matched-pairs signed-rank test was performed on %CSR and RT at days 28 and 84.

2.5. MRI acquisition

MRI data were acquired on a single 3T Siemens Skyra^{fit} scanner (Siemens Healthcare, Erlangen, Germany) equipped with a 16-channel receive head and neck coil and using Syngo MR E11 software before training (baseline), during training at 7, 14 and 28 days, and at 84 days follow-up. If scanning and training were scheduled on the same day, the training took place after the scan. These time points were selected based on timescale over which the task was expected to induce significant performance improvement (Höysniemi, 2006; Kearney, 2008) and the observed trajectories of induced plasticity in the MRI literature (Draganski et al., 2006; Kodama et al., 2018; Makino et al., 2016).

All participants underwent an MPM protocol to furnish estimates of R1, MT_{sat} and $R2^*$ (Helms and Dechent, 2009; Leutritz et al., 2020; Weiskopf et al., 2013, 2011a). The MPM protocol acquires three volumes using a 3D multi-echo spoiled gradient echo sequence (based on the Siemens FLASH product sequence) with 1 mm^3 isotropic resolution and a field of view (FoV) of $240 \times 256 \times 176$ mm^3. Each volume was acquired using a different TR and radio-frequency (RF) excitation flip angle combination to achieve images with either T1-weighting: 25 ms / 23°, proton density (PD)-weighting: 25 ms / 4°, or MT-weighting: 37 ms / 9°, with an off-resonance MT_{sat} pulse applied prior to excitation. Echoes were acquired at 6 equidistant echo times (TE) from 2.46 to 14.76 ms for all weightings, with an additional 2 echoes at 17.22 and 19.68 ms for the PD-weighted and T1-weighted volumes. Total acquisition time was 23 mins. We used parallel imaging with an acceleration factor of 2 in both phase-encoding directions. Subsequent reconstruction was performed with the generalised auto-calibration partially parallel acquisition algorithm (GRAPPA) in the anterior-posterior phase-encoding direction and a partial Fourier acquisition with a 6/8 sampling factor in the partition direction left-right.

2.6. MRI processing

A total of five scans were acquired for each participant. MPM maps were generated with the hMRI toolbox v0.2.0 (Tabelow et al., 2019) in SPM12 (Wellcome Trust Centre for Neuroimaging, London, UK, http://www.fil.ion.ucl.ac.uk/spm) and Matlab, using UNICORT (Weiskopf et al., 2011) to correct for transmit field inhomogeneities (Emmenegger et al., 2021). All maps were pre-processed using an analysis pipeline for longitudinal data (Ziegler et al., 2018), in which MT_{sat} maps were first skull-stripped. For skull-stripping, the MT_{sat} maps were segmented using the "Segment Longitudinal Data" of the CAT12 toolbox (CAT12.6 (r1450) http://www.neuro.uni-jena.de/cat/) with the graph-cut/region-growing (GCUT) approach. After this skull-skipping step, the MT_{sat} maps were used for longitudinal registration within-participants, based on a generative model, in which each image volume was registered to a subject-specific average map, combining non-linear and rigid-body registration with corrections for intensity bias artefacts (Ashburner, 2013). This procedure generated participant-specific, midpoint maps with corresponding deformation fields.

Second, a unified segmentation was applied to the subject's midpoint map, generating probability maps of GM, WM, and cerebrospinal fluid (CSF) (Ashburner and Friston, 2005). Third, nonlinear template generation and image registration was applied to subject-specific, midpoint GM and WM tissue maps based on Dartel (Ashburner, 2007) and the resulting template was registered to Montreal Neurological Institute (MNI) space using an affine transform. Fourth, all MPM maps were warped to MNI space using the transformations obtained in the previous steps. Finally, all MPM maps in MNI space were spatially smoothed using a Gaussian kernel with 5-mm (in GM) and 3-mm (in WM) full-width at half-maximum (FWHM) while appropriate tissue segment weighting was used to minimise partial volume effects of GM/WM (Draganski et al., 2011).

To relate the quantitative MPM metrics to conventional morphometric approaches (such as voxel-based morphometry [VBM]), MT_{sat} maps were additionally pre-processed using the longitudinal VBM analysis from CAT12 toolbox. This longitudinal VBM analysis includes the realignment of all time points for each subject using an inverse-consistent rigid registration, which includes bias-correction before the realigned MT_{sat} are segmented into GM, WM and CSF. Next, deformation fields to the MNI space were computed using a non-linear spatial registration (Dartel) (Ashburner, 2007). The resulting deformations were applied to the tissue segmentations (GM and WM probability maps) at all time points, modulated with the Jacobian determinant of the deformation and spatially smoothed using isotropic Gaussian smoothing of 6-mm (in the GM) and 4-mm (in the WM) FWHM. For statistical analysis, we excluded all voxels with a GM probability below 0.2 and WM probability below 0.6 to minimise contribution from partial volume effects near GM/WM borders. Quality assessments were conducted after each processing step using the quality assessment function in CAT12 and visual inspections by imaging experts. One non-trained participant was excluded from the VBM analysis due to mis-segmentation. For the quantitative MPM maps, no subject data had to be excluded after quality assessment.

2.7. MRI statistics

2.7.1. Regions of interest

We first ran a whole brain analysis for explorative purposes and then used a hypothesis-driven region of interest (ROI) analysis to focus the analysis of training-related changes in brain (micro-) structure and for subsequent tests for coherent patterns of changes across ROIs and time (see further methods sections). The ROIs were chosen based on prior studies reporting GM and WM changes in response to upper and lower limb training (Boyke et al., 2008; Draganski et al., 2006; Hüfner et al., 2011; Lakhani et al., 2016; Schlegel et al., 2012; Scholz et al., 2009; Wenger et al., 2016) and represented the networks likely to be recruited by the various elements of the task including consolidation of motor sequence learning (Long et al., 2018). These comprised the sensorimotor cortices (M1), cranial corticospinal tract (CST), thalamus, cerebellum, and the hippocampal formation comprising the entorhinal cortex (EC) and the hippocampus with the dentate gyrus, cornu ammonis, and subiculum. The hippocampal formation and CST were defined based on the Oxford Centre for Functional MRI of the Brain Software Library (FSL) templates in MNI space; while sensorimotor cortices, thalamus, and cerebellum were defined using the anatomy toolbox in SPM (Eickhoff et al., 2007, 2005). These regions were also combined into one ROI for each hemisphere and tissue type (GM/WM).

2.7.2. Training-induced structural changes

We used SPM to assess the following within the predefined ROIs: (i) training-induced brain changes; (ii) topological changes and (iii) how training improvements (in terms of δ and γ from the behavioural analysis) were related to structural trajectories. The model for the training-induced brain changes and topological changes incorporated an intercept and a linear and quadratic time effect for each subject sepa-

Table 1
Longitudinal SPM shows differences of the linear and quadratic time dependence in myelin-sensitive longitudinal relaxation rate (R1) and magnetisation transfer rate (MT_{sat}), and transverse relaxation rate ($R2^*$) maps between trainees and untrained healthy controls. *R*=right, *L*=left.

ROI	MAP	Contrast	Cluster size	p value (FWE-corrected)	z-value	x[mm]	y[mm]	z[mm]
Cerebellum L	MT_{sat}	quadr Trained > NonTrained	271	0.008	4.36	−19.5	−39	−55.5
Hippocampus R	MT_{sat}	quadr Trained > NonTrained	192	0.032	4.29	25.5	−3	−24
Corticospinal tract L	MT_{sat}	quadr Trained > NonTrained	77	0.049	3.85	−13.5	−21	−13.5
Corticospinal tract R	MT_{sat}	quadr Trained > NonTrained	90	0.045	3.94	16.5	−13.5	4.5
Cerebellum L	R1	quadr Trained > NonTrained	362	0.015	4.36	−6	−67.5	−54
Cerebellum R	$R2^*$	linear Trained < NonTrained	139	0.043	3.72	30	−37.5	−27
Cerebellum R	$R2^*$	quadr Trained > NonTrained	202	0.011	3.77	10.5	−55.5	−7.5

rately. The general linear model included predictors (intercept, time, $time^2$) and covariates (age, total intracranial volume [TIV]). The time and $time^2$ parameters were mean-centred and the linear component was orthogonalised with respect to the quadratic component, enabling the identification of both linear and transient negative quadratic (low-high-low) and transient positive quadratic (high-low-high) trajectories (Ziegler et al., 2018). Training-induced brain changes were defined as the difference between the combined trained (upper + lower limb training groups) and the untrained group. The same model was used to assess somatotopic effects comparing lower-limb with upper-limb trainees in the same ROIs.

To analyse the association between MRI and motor learning parameters, we used SPM's multiple linear regression models to test for associations between linear and quadratic structural changes (linear or quadratic beta from each subject) with behavioural improvement (δ), and speed of improvement (γ), for each participant-specific model, using both training parameters (%CSR and RT). For this association analysis, we have excluded parameters exceeding the three standard deviations from the group mean. These variates allowed us to assess if linear or quadratic brain changes were associated with training improvements. All results with family-wise error (FWE) corrected p-value below 0.05, and a cluster size ≥ 20 was considered significant.

2.7.3. Coherent changes in microanatomy within the corticospinal and hippocampal systems

To investigate coherent changes (i.e., changes in different brain regions correlated at the same time point or time-lagged changes at subsequent time points) in structural metrics within and between sub-cortical and cortical areas of interest, mean microstructural values from the significant MT_{sat} group comparison clusters were extracted from the maps in MNI space for all trained participants. In the time-lagged analyses, for each group mean MRI parameter in a given cluster, correlation was assessed using a mixed-effects model correcting for age and TIV with the same cluster and parameter at the next timepoint in the training period (i.e. baseline, days 7, 14 and 28). This analysis was performed between motor areas (CST and cerebellum) and the hippocampus to investigate if the motor areas or hippocampal consolidation occurs first when responding to training. In other words, we looked for correlations between changes in one cluster (e.g. mean MT_{sat} from the left CST) with time-lagged changes in another (e.g. mean MT_{sat} from right hippocampal formation at the subsequent time point). Coherent but not time-lagged (i.e. between different clusters at the same timepoint) changes were further assessed within the motor areas.

3. Results

3.1. Demographics and behavioural results

The three training groups did not significantly differ with respect to age (upper limb training [n = 9, age=34.48±10.94 SD years]; lower limb training [n = 9, age=39.17±14.07 SD years]; no training [n = 14, age=38.89±11.18 SD years; ANOVA: F = 0.46, p = 0.64]). All trained participants improved (in terms of δ) in both %CSR (p<0.001, z = 3.72) and RT (p<0.001, z = 3.72) over the 28 days of training (Fig. 1E). At baseline, the combined group of trained participants achieved 76.75 %CSR (interquartile range [IQR]: 69.11 – 90.38%) improving by a median of 18% (IQR: 11 – 23%) by 18 days (time = $3/\gamma$ for 95% improvement, with γ = 0.17, IQR: 0.11–0.26). Median RT was 55.8 ms (IQR: 45.71 – 63.04 ms) at baseline, and trained participants improved by a median 25.77 ms (IQR: 15.00 – 34.82) reaching a plateau at 18 days (time = $3/\gamma$ for 95% improvement, with γ= 0.17, IQR: 0.10 – 0.28).

At baseline, lower limb trainees achieved 69.11 %CSR (IQR: 61.78 – 75.16) and RT was 58.83 ms (IQR: 53.35 – 63.04); while upper limb trainees achieved 90.38%CSR (IQR: 87.73 – 90.76%, p = 0.001) with a RT of 50.57 ms (IQR: 40.57 – 60.93 ms; Fig. 1F, p = 0.171). This allowed participants training the lower limbs to improve more in terms of %CSR (22% [IQR: 22 – 29] versus 11% [IQR: 9 – 12]) compared to upper-limb trainees (p = 0.004, two-tailed test), while improvement in RT was similar between the groups (lower limb: 30.05 ms, [IQR: 13.8 – 34.82] versus upper limb: 25.4 ms, [IQR: 22.58 – 28.4], p = 0.895, two-tailed test).

Specific improvements in %CSR and RT for inputs exclusively delivered by the left or right side were not significantly different (p>0.05, two-tailed test). Between days 28 and 84, no significant differences between %CSR and RT were observed (p = 0.930 and p = 0.349 respectively). In summary, the training task led to rapid and sustained performance improvements in both the upper and lower limb trainees.

3.2. Volumetric and microstructural responses to training

3.2.1. Whole brain

At baseline, there were no differences in any MRI metric between trainees and non-trainees. Using an exploratory whole brain GM and WM approach (supplementary material 2 A-E) we observed greater quadratic WM volume changes in the right corona radiata (quadratic cluster 1: z = 5.20, p = 0.034) and left prefrontal WM (z = 6.46, p<0.001) in trainees compared to non-trainees. Trainees also showed greater positive quadratic R1 changes in the right hippocampus (z = 3.872, p = 0.007), as well as greater negative linear $R2^*$ changes in the left corona radiata (z = 3.833, p = 0.021).

3.2.2. ROI based analysis

At baseline, there were no differences in any MRI metric in any ROI between trainees and non-trainees. In the left posterior cerebellum, trainees showed greater positive quadratic changes in myelin markers than non-trained participants (MT_{sat}: z = 4.362, p = 0.008; R1: z = 4.361, p = 0.015, Table 1, Figs. 2A&B). Trainees also showed greater positive quadratic MT_{sat} changes (z = 4.292, p = 0.032, Table 1, Fig. 2C) in the right hippocampal formation and in the bilateral CST (left: z = 3.853, p = 0.049; right: z = 3.939, p = 0.045, Table 1, Fig. 2D). In the right anterior cerebellum, trainees showed greater negative linear and positive quadratic $R2^*$ changes than non-trained participants (linear: z = 3.718, p = 0.043; quadratic: z = 3.765, p = 0.011 Table 1, Fig. 2E&F). In summary, training-induced microstructural changes occurred in cortical and subcortical structures and involved GM as well as WM changes.

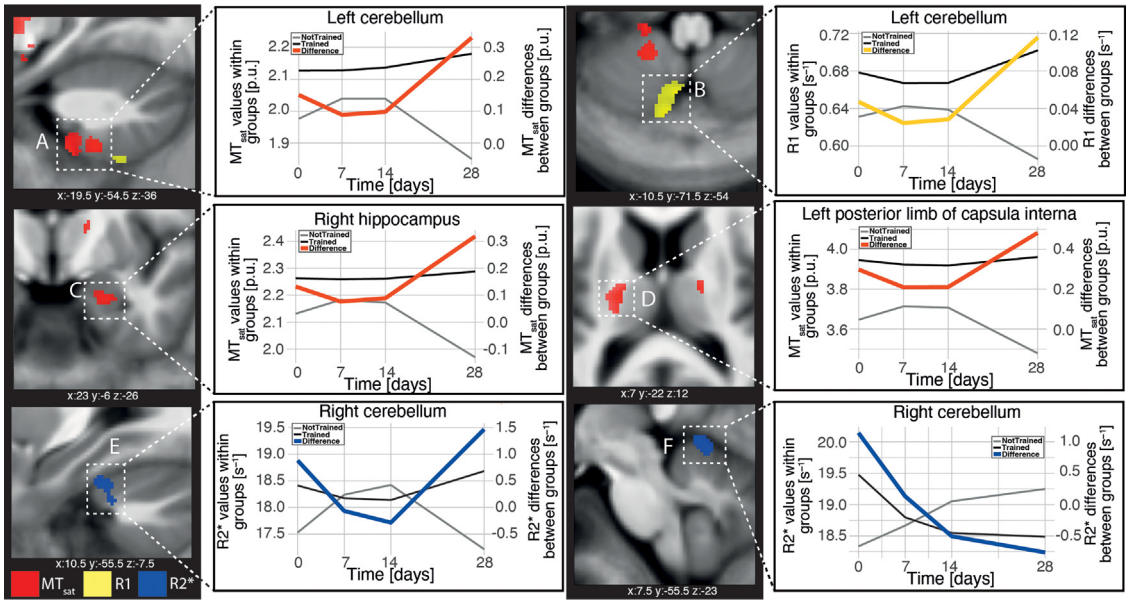

Fig. 2. Training-induced changes during learning of the motor skill task (upper and lower limb combined) when compared to untrained healthy controls. Positive quadratic magnetization transfer saturation (MT_{sat}) changes [red] were observed in the (A) left cerebellum, (C) right hippocampal formation, and (D) left corticospinal tract at the level of the internal capsule. Positive quadratic longitudinal relaxation rate (R1) [yellow] (B) and transverse relaxation rate (R2* [blue]) (E&F) were observed in the cerebellum.

Table 2
Correlations between the linear and quadratic time dependence in transverse relaxation rate (R2*) maps and response time (RT) improvement. *R*=right, *L*=left.

ROI	MAP	Contrast	Cluster size	p value (FWE-corrected)	z-value	x[mm]	y[mm]	z[mm]
Cerebellum posterior part L	R2*	positive correlation between linear change and RT improvement	202	0.007	5	−43.5	−54	−46.5

Table 3
Longitudinal SPM analysis showing differences of the linear and quadratic time dependence myelin-sensitive transverse relaxation rate (R2*) and magnetisation transfer rate (MT_{sat}) maps between upper limb trainees and lower limb trainees. *R*=right, *L*=left.

ROI	MAP	Contrast	Cluster size	p value (FWE-corrected)	z-value	x[mm]	y[mm]	z[mm]
Thalamus L	MT_{sat}	linear Upper > Lower	178	0.038	3.499	−15	−15	9
Thalamus R	MT_{sat}	linear Upper > Lower	267	0.010	3.712	10.5	−13.5	10.5
Corticospinal tract L	MT_{sat}	linear Upper > Lower	251	0.001	4.339	−24	−12	−7.5
Thalamus R	R2*	Quadr Upper > Lower	158	0.028	4.668	18	−34.5	−1.5

3.3. Associations with performance improvements

3.3.1. Whole brain

Using an exploratory whole brain GM and WM approach, we observed a positive association between quadratic WM changes in the left corona radiata and RT improvement ($z = 3.88$, $p = 0.001$, supplementary material 2 D).

3.3.2. ROI based approach

Faster response time (RT) improvement (δ) was positively correlated with linear R2* changes in the left posterior part of the cerebellum ($z = 5.000$, $p = 0.007$; Table 2 and Fig. 3).

3.4. Somatotopy of lower vs. upper limb training

In the bilateral thalamus, upper limb trainees showed larger linear MT_{sat} changes (left $z = 3.499$, $p = 0.038$; right $z = 3.712$, $p = 0.010$; Fig. 4A and Table 3) than lower limb trainees. Upper limb trainees also showed greater transient quadratic R2* changes in the right thalamus ($z = 4.668$, $p = 0.028$, Fig. 4A and Table 3) than lower limb trainees. In the CST, upper limb trainees showed greater magnitude linear MT_{sat} changes in the left posterior limb of the internal capsule (MT_{sat}: $z = 4.339$, $p = 0.001$; Fig. 4B and Table 3),

3.5. Coherent changes in microstructure within the cranial corticospinal tract, hippocampal and cerebellar systems

There was a positive correlation between the bilateral CST and left cerebellum in terms of MT_{sat} changes (Fig. 5 and Table 4). In the time-lagged analyses, at any given timepoint, there was a positive correlation between changes in MT_{sat} in the left CST and changes in MT_{sat} in the right hippocampus at the following time point ($p = 0.001$, Fig. 5 and Table 4). Further, the MT_{sat} changes in the right CST were positively correlated with the right hippocampus at the following time point ($p = 0.027$, Fig. 5 and Table 4).

4. Discussion

This study provides novel insights into the nature of (micro-)structural brain changes accompanying skill acquisition in the motor

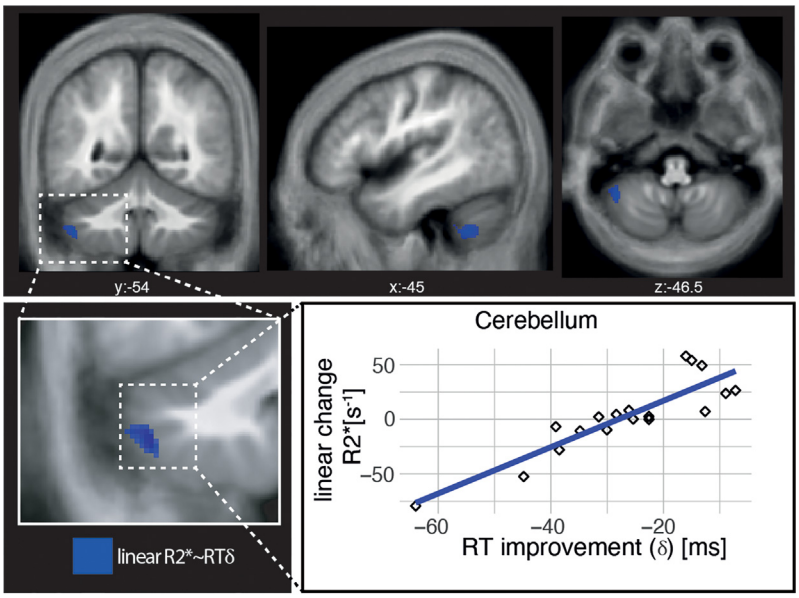

Fig. 3. Associations between linear transverse relaxation rate (R2*) changes and training improvements in response time (i.e. reduction [δ] of in response time [RT]) in the left cerebellum. Note that the scatter graphs depicts the model average in the significant cluster with an approximation of linear change for individual subjects.

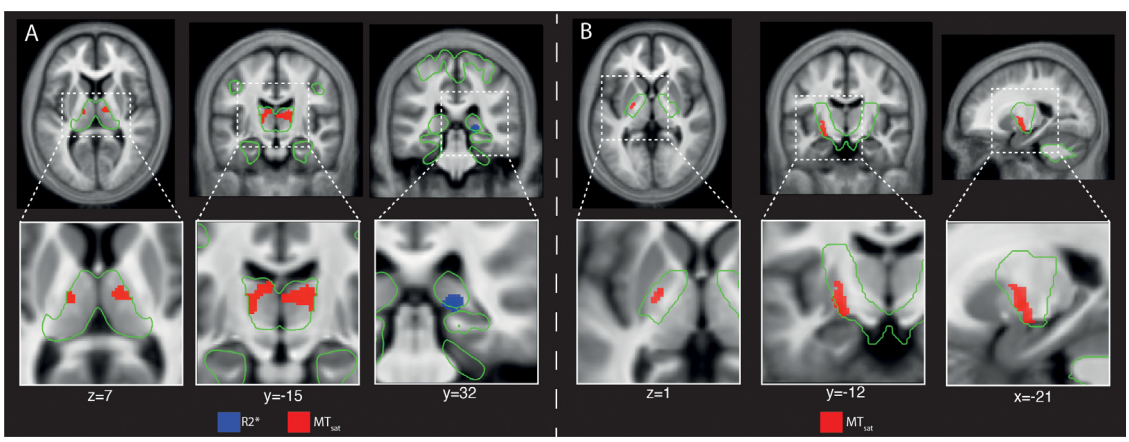

Fig. 4. Somatotopic differences associated with training the upper vs. lower limbs. (A) Upper limb training resulted in a greater linear change in magnetisation transfer (MT_{sat}; red) in the bilateral upper limb area of the thalamus, while this was observed only on the right side for transverse relaxation rate (i.e. quadratic R2*; blue), when compared to lower limb training. (B) Training of the upper limbs resulted in greater linear change in MT_{sat} in the upper limb area of the left corticospinal tract compared to lower limb training. Superimposed in green is the outline of the region of interest (ROI).

Table 4
Table showing the results from the in time and time lag analysis for magnetisation transfer rate (MT_{sat}) within the corticospinal tracts, cerebellum and hippocampal formation.

Map temporal association	Coefficient	Standard error	z value	p value	95% Confidence interval
Correlated in time					
Left corticospinal tract (MT_{sat}) and left cerebellum (MT_{sat}) in time	0.307	0.073	4.19	<0.001	0.164 – 0.451
Right corticospinal tract (MT_{sat}) and left cerebellum (MT_{sat}) in time	0.209	0.079	2.65	0.008	0.054 – 0.363
Left corticospinal tract (MT_{sat}) and right corticospinal tract (MT_{sat}) in time	0.920	0.060	15.43	<0.001	0.803 – 1.037
Correlated with a time shift of one prior timepoint					
Left corticospinal tract (MT_{sat}) with the right hippocampus (MT_{sat}) at the following timepoint	0.623	0.194	3.22	0.001	0.243 – 1.002
Right corticospinal tract (MT_{sat}) with the right hippocampus (MT_{sat}) at the following timepoint	0.510	0.231	2.21	0.027	0.058 – 0.962

learning game StepMania. Amongst trainees, microstructural changes in the corticospinal, cerebellar and hippocampal system revealed an intricate interplay across networks and time, including both transient and persisting changes, the magnitude of which was associated with performance improvements. Furthermore, an upper versus lower limb somatotopy was reflected by myelin-sensitive MT_{sat} and iron-sensitive R2* changes in the thalamus and the CST at the level of the posterior limb of the internal capsule. Taken together, these findings offer support for some of the putative neuroplastic mechanisms that underwrite motor learning—with potentially transferable insights for motor rehabilitation and clinical practice.

4.1. The trajectories of microstructural responses to training

R1 and MT_{sat} are increasingly accepted as surrogate markers of myelin content (Georgiadis et al., 2021; Natu et al., 2019; Schmierer et al., 2004) while R2* is known to be highly sensitive to iron deposition (Ghadery et al., 2015; Langkammer et al., 2010; Natu et al.,

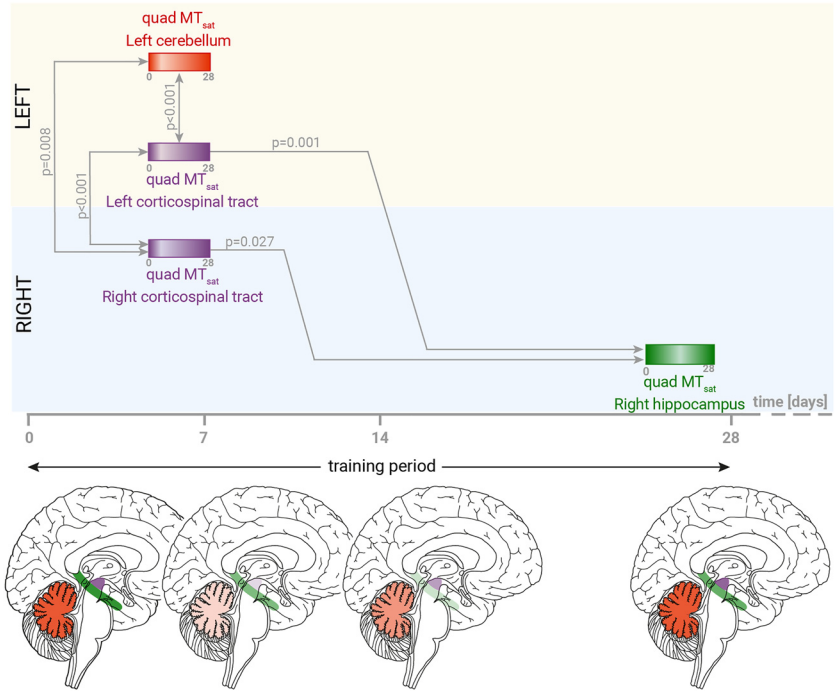

Fig. 5. Schematic representation of the coherent changes in magnetisation transfer saturation (MT_{sat}) between corticospinal tract (purple), hippocampus (green) and cerebellum (red), over time during training. Single-headed arrows indicate the time-shifted analysis indicating the temporal time lag between two brain structures, whereas a double-headed arrow indicates the correlation in time between both brain areas. Gradient colour changes within the boxes and brain indicate the evolution of the convex course of non-linear changes observed across time.

2019). Over 1 month of active training, we observed tissue-specific transient R1, MT_{sat} and R2* changes in key, specific brain areas associated with motor-skill learning (Dayan and Cohen, 2011; Draganski and May 2008; Zatorre et al., 2012) across the corticospinal, cerebellar and hippocampal systems. Most of these microstructural markers of myelin and iron initially decreased between days 7 and 14 and renormalised by day 28 (Fig. 2).

The hippocampus is capable of plastic change in response to various tasks—reflecting its diverse roles—with volume increases associated with motor learning in mice (Badea et al., 2019) and acquired expertise in human navigation, dancing and juggling in volumetric GM analyses (Boyke et al., 2008; Hüfner et al., 2011). A key element of performance improvement in StepMania is the translation of complex cue patterns into optimal motor response sequences, which are based on experience of the task and a degree of mnemonic sequence learning. The hippocampus is known to encode visuospatial memories and is active in early and later implicit and explicit motor sequence learning (Gheysen et al., 2010; Long et al., 2018) and in offline reprocessing of prior learning (Albouy et al., 2008; Jacobacci et al., 2020; Pinsard et al., 2019), which is enhanced by sleep (Pinsard et al., 2019). In patients with right medial temporal lobe epilepsy, better performance in a motor sequence tapping task was associated with larger anterior hippocampal volume (Long et al., 2018). The transient positive quadratic trajectories in MT_{sat} that we observed during training in the hippocampus may be explained by dilutive activity-induced angiogenesis (Erickson et al., 2011) or myelin remodelling (Bacmeister et al., 2021) in these dense GM regions, or by classical Hebbian propagation, stabilisation and elimination of dendritic spines. Crucially, somatotopic analysis revealed differences in the magnitude of microstructural changes between upper and lower limb trainees in the posterior limb of the internal capsule. This is in keeping with somatotopic anatomy of the upper and lower limb in the CST (Purves et al., 2018; Schneider et al., 1994), where upper limb fibres are located anteriorly (Purves et al., 2018) and the lower limb fibres dorsally (Schneider et al., 1994). These findings highlight the sensitivity of these MPM analyses to discriminate relatively small, functionally important areas with clear potential as a neuroimaging biomarker for limb-specific rehabilitation or therapeutic interventions.

At the whole brain level, we found R2* and volumetric changes in the corpus callosum and the corona radiata, respectively. Both contain fibre tracts that are critically implicated in motor control. The corpus callosum connects the two hemispheres and is critical for tasks that require interhemispheric communication, while the corona radiata is the anatomical linkage that supports cognitive and perceptual and motor systems in the cortex – all aspects involved in motor skill learning. This notion is supported by our finding that greater transient volume changes in the corona radiata are correlated with better reaction time improvement.

In the behavioural analysis, performance improvement in StepMania was accompanied by linear R2* changes in the left cerebellum. Abundant projections between the lateral cerebellum and sensorimotor cortical regions underlie the former's role in many aspects of motor control, including visuospatial cognition (Brissenden et al., 2018; Burciu et al., 2013) and the anticipatory postural adjustments required for mastery of StepMania. These results parallel findings from prior VBM experiments, in which GM volume increases were seen in the cerebellum in patients with Parkinson's disease (Sehm et al., 2014) and healthy individuals (Burciu et al., 2013) during the learning of different postural motor control tasks, or in professional basketball players compared to healthy controls (Park et al., 2009).

4.2. Temporal dynamics of multimodal changes across subcortical and cortical regions

Acquiring five serial scans per subject afforded the opportunity to assess temporal associations between microstructural changes across subcortical and cortical areas constituting the cortico-cerebellar-hippocampal networks involved in task learning. This approach, uniquely augmented with MPM, is exploratory. Three key interdependencies were revealed in the microstructural data. Firstly, our findings suggested that transient changes in the left and right hemispheres are correlated at a given timepoint, as would be expected in a bimanual / bipedal task. Secondly, transient decreases in MT_{sat} in the CST are linked to later, similarly transient decreases in MT_{sat} in the right hippocampus. This suggests that the fine-tuning / optimisation of learning of a motor skill by the cerebellum and corticospinal tracts is prior to its consolidation in the hippocampus.

As the CST and hippocampal formations share only limited direct connections (Burman, 2019; Maller et al., 2019), we assume that these changes represent two separate but associated aspects of learning whereby the cortico-cerebellar loop subtends fine-tuning of movement

and the hippocampus is responsible for consolidation of learning. Contemporaneous volumetric increases have been observed in the sensorimotor cortex and the hippocampus during 5 days of visuo-motor training (Kodama et al., 2018), but this is the first evidence of a corticospinal-cerebellar-hippocampal circuit active during motor learning and underlines the potential utility of quantitative MRI markers in mapping skill acquisition and recovery over time.

4.3. Neurobiology underpinning imaging outcomes related to training

The biological processes underpinning motor learning in humans remain hotly debated and are likely multifactorial, with candidate mechanisms including synaptogenesis, angiogenesis, gliogenesis, or myelin remodelling (Adams et al., 1997; Blumenfeld-Katzir et al., 2011; Canu et al., 2009; Dong and Greenough, 2004; Fields, 2015; Kleim et al., 2002; Pereira et al., 2007; Rhyu et al., 2010; Ruegg et al., 2003; Sampaio-Baptista et al., 2020, 2013; Sampaio-Baptista and Johansen-Berg, 2017; Toscano-Silva et al., 2010; Tronel et al., 2010; Yang et al., 2009; Yasuda et al., 2011; Zatorre et al., 2012). During synaptogenesis in the GM, an initial decrease in the myelin markers R1 and MT_{sat} may be expected, as the relative proportion of myelin decreases due to new, unmyelinated connections. In parallel, a reduction in $R2^*$ should be observed, as iron is consumed during synaptogenesis (Carlson et al., 2007; Tran et al., 2015). These processes are followed by a pruning phase (Kantor and Kolodkin, 2003; Yasuda et al., 2011) during which redundant connections are eliminated and activity-dependant myelination of new connections takes place, increasing the relative myelin proportion (Fields, 2015; Sampaio-Baptista and Johansen-Berg, 2017), while iron deposition also results in $R2^*$ increases (Möller et al., 2019; Weiskopf et al., 2021). However, synaptogenesis is unlikely to play a significant role in WM tracts, where we observed similar effects.

Myelin remodelling in the presence or absence of significant synaptogenesis may also explain the trajectories observed in both GM and WM. Myelin changes were suggested most strongly by transient MT_{sat} changes in the cerebellum, internal capsule and the hippocampus of trainees and R1 changes elsewhere in the cerebellum. Oligodendrogenesis, the generation of oligodendrocyte precursor cells responsible for myelination, has been observed in recruited brain regions in trained rodents (Gibson et al., 2014) and the absence of oligodendrogenesis leads to impaired motor skill learning (McKenzie et al., 2014). In adult humans, the oligodendrocyte population is stable with a low turnover rate, suggesting myelination in response to training in adulthood is carried out at least in part by mature oligodendrocytes (Bacmeister et al., 2021; Yeung et al., 2014). A recent publication provides compelling evidence of a staged response to motor training in the M1 of adult mice, whereby pre-existing myelin sheaths of behaviourally activated axons retract in the early stages of motor learning before a period of new myelination as learning is consolidated (Bacmeister et al., 2021). While these preliminary findings are in keeping with the trajectories in myelin-sensitive MR parameters observed in this study, further mechanistic studies are required to determine if and to what degree our findings are reflective of underlying neural and/or myelination processes.

Alternatively, dynamic changes in MT_{sat}, R1 and $R2^*$ may represent a relatively reduced proportion of myelin due to training-induced angiogenesis or gliogenesis (Badea et al., 2019; Fields, 2015) and are in keeping with the early literature on local tissue volume expansion in response to training (Draganski and May 2008; Zatorre et al., 2012). Transient vasculature changes have been demonstrated in vivo where physical exercise induced a temporary, histologically-confirmed increase in vascular volume in the adult simian M1 (Rhyu et al., 2010), although human neuroimaging studies analysing cerebral blood volume did not corroborate this (Thomas et al., 2016). As both angiogenesis and gliogenesis are based on changes in non-neural substrates common to both GM and WM, either or both could underlie the transient changes observed.

4.4. Limitations

While increasingly accepted as a proxy for CNS microstructure and well-correlated with histological myelin markers (Clayden et al., 2015; Natu et al., 2019), R1, $R2^*$ and MT_{sat} remain indirect estimates of microstructure. However, we were able to demonstrate coherent changes consistent with the current understanding of the processes underpinning complex motor learning tasks (Lungu et al., 2014). Selecting an optimal training task for such a study is a compromise, and we faced the additional difficulty of requiring a task that was relevant and challenging, yet achievable, for patients with neurological deficits and healthy participants alike. The training duration of 4 weeks was chosen based on prior studies (Draganski et al., 2006; Makino et al., 2016) and this choice was validated by the fact that almost all participants achieved asymptotic performance in the third or final week of training. The data gathered here will be used in future studies in comparison to patients with neurological injury learning StepMania as a rehabilitation activity. It is for this reason that participant allocation was randomised with age-matching to ensure comparability with patients with spinal cord injury. While this offers less protection against other confounding differences, such as body weight, these confounds are minimised using an exclusively male, right-handed population, for which intra-scanner coefficient of variation for MPM parameters on our scanner has been determined to be <5% (Leutritz et al., 2020). Analyses in this study were limited to linear and quadratic temporal changes, although clearly other temporal patterns are possible. The quadratic model has been previously utilised (Wenger et al., 2016) and is particularly suitable for the detection of expansion and renormalisation processes in the brain during learning (Draganski et al., 2006; Hopkins et al., 2018; Moraud et al., 2016). In some quantative MRI metrics in some brain ROIs, we observed simple main effects of time in the untrained control group. These effects may be due to factors such as hydration, sleep or head positioning, which have been shown to affect traditional morphological metrics such as local GM volume. For example, patients with sleep disorders have reduced GM in various brain regions, including the hippocampal formation, compared to normal sleepers (Campabadal et al., 2021). Dehydration may also cause GM volume decreases (Streitbürger et al., 2012). In this study, scans were acquired on weekdays at similar times and never after training. However, systematic changes in sleep patterns and hydration are difficult to fully exclude. Further, the non-trained group was instructed not to acquire any new skills and specifically not to take dance lessons, but to continue with their previous habits. The requirement to attend scans may have resulted in a reduction in overall daily activity that was not controlled for in the training group, and this could potentially lead to structural brain changes (Langer et al., 2012). Quantitative MRI generally shows higher specificity, which may come at the cost of locally-elevated noise levels (Edwards et al., 2018; Freund et al., 2019). While the use of UNICORT has been shown to reduce transmit field inhomogeneities (Callaghan et al., 2015; Weiskopf et al., 2011), it may decrease accuracy (Emmenegger et al., 2021), rendering e.g. MT_{sat} changes ≤1.4% indistinguishable between trained and non-trained subjects. However, under the assumption that group assignment was randomised (with age-matching), the significant group trajectory differences (i.e., the interaction between group and time) can be attributed to the effects of motor training.

5. Conclusion

Serial quantitative MRI parameters were acquired in healthy individuals learning to master the motion game StepMania using either their upper or lower limbs. Analysis revealed multimodal changes across the corticospinal, cerebellar and hippocampal systems in trainees. Microstructural markers sensitive to myelin and iron content followed transient courses, consistent with myelin remodelling and / or local tissue composition changes. Somatotopic differences in the magnitude of changes in myelin-sensitive markers were observed between the upper

and lower limb training groups in the CST suggesting a somatotopy of learning, whereby activity dependant myelin modelling results in strengthened connections and / or faster conduction velocities. When we correlated microstructural changes across regions and timepoints, evidence of a coherent and choreographed motor learning network active during motor skill learning in healthy individuals was revealed, encompassing the CST, cerebellum and hippocampal formation. Taken together, these results offer insights into the co-ordinated plasticity of a corticospinal-hippocampal-cerebellar network, accessible with non-invasive MRI, subtending skill acquisition in the undamaged brain.

CRediT author statement

Michela Azzarito: Conceptualisation, Methodology, Analysis, Writing first draft; **Tim Emmenegger:** Methodology, Analysis, Editing draft; **Gabriel Ziegler:** Conceptualisation, Methodology, Analysis, Editing draft; **Eveline Huber:** Conceptualisation, Methodology, Analysis, Editing draft; **Patrick Grabher:** Conceptualisation, Methodology, Analysis, Editing draft, **Martina F. Callaghan:** Conceptualisation, Methodology, Editing draft; **Alan Thompson**: Conceptualisation, Editing draft; **Karl Friston**: Conceptualisation, Methodology, Editing draft; **Nikolaus Weiskopf:** Conceptualisation, Methodology, Editing draft; **Tim Killeen**: Conceptualisation, Methodology, Analysis, Writing first draft, Editing draft and **Patrick Freund**: Conceptualisation, Methodology, Analysis, Editing draft.

Funding

This work was supported by Wings for Life, Austria (WFL-CH-007/14). PF is funded by a SNF Eccellenza Professorial Fellowship grant (PCEFP3_181362 / 1). Open access of this publication is supported by the Wellcome Trust (091593/Z/10/Z). NW has received funding from the European Research Council under the European Union's Seventh Framework Programme (FP7/2007–2013) / ERC grant agreement 616,905; from the BMBF (01EW1711A & B) in the framework of ERA-NET NEURON. PF and NW have received funding from the European Union's Horizon 2020 research and innovation programme under the grant agreement No 681094.

Declaration of Competing Interest

None.

Data availability

Anonymised grouped data will be shared on request from a qualified investigator.

Acknowledgments

We would like to thank all participants for participation in this study. We thank Eric Reese (https://github.com/kyzentun) for selflessly offering his time and expertise in the writing of the StepMania scripts. We also thank Dr Maryam Seif, Prof Bogdan Draganski, Dr. Chris Easthope Awai, Dr. Marc Bolliger and Prof. Armin Curt for their guidance and support in developing and carrying out this study; and thanks to Daniel R. Altmann for the statistical support.

Supplementary materials

Supplementary material associated with this article can be found, in the online version, at doi:10.1016/j.neuroimage.2023.120128.

References

Adams, B., Lee, M., Fahnestock, M., Racine, R.J., 1997. Long-term potentiation trains induce mossy fiber sprouting. Brain Res. 775, 193–197. doi:10.1016/S0006-8993(97)01061-5.

Albouy, G., Sterpenich, V., Balteau, E., Vandewalle, G., Desseilles, M., Dang-Vu, T., Darsaud, A., Ruby, P., Luppi, P.-H.H., Degueldre, C., Peigneux, P., Luxen, A., Maquet, P., 2008. Both the hippocampus and striatum are involved in consolidation of motor sequence memory. Neuron 58, 261–272. doi:10.1016/j.neuron.2008.02.008.

Ashburner, J., 2007. A fast diffeomorphic image registration algorithm. Neuroimage 38, 95–113. doi:10.1016/j.neuroimage.2007.07.007.

Ashburner, John, 2013. Symmetric Diffeomorphic Modeling of Longitudinal Structural MRI. Frontiers in Neuroscience 6 (FEB):, 197. doi:10.3389/fnins.2012.00197.

Ashburner, J., Friston, K.J., 2005. Unified segmentation. Neuroimage 26, 839–851. doi:10.1016/j.neuroimage.2005.02.018.

Bacmeister, C.M., Huang, R., Thornton, M.A., Conant, L., Chavez, A., Poleg-polsky, A., Hughes, E.G., 2021. Motor learning drives dynamic patterns of intermittent myelination on learning-activated axons. bioRxiv Prepr. doi:10.1101/2021.10.13.464319.

Badea, A., Ng, K.L., Anderson, R.J., Zhang, J., Miller, M.I., O'Brien, R.J., 2019. Magnetic resonance imaging of mouse brain networks plasticity following motor learning. PLoS One 14, 1–21. doi:10.1371/journal.pone.0216596.

Blakemore, S.J., Wolpert, D.M., Frith, C.D., 1999. The cerebellum contributes to somatosensory cortical activity during self-produced tactile stimulation. Neuroimage 10, 448–459.

Blumenfeld-Katzir, T., Pasternak, O., Dagan, M., Assaf, Y., 2011. Diffusion MRI of structural brain plasticity induced by a learning and memory task. PLoS One 6, e20678. doi:10.1371/journal.pone.0020678.

Boyke, J., Driemeyer, J., Gaser, C., Buchel, C., May, A., 2008. Training-induced brain structure changes in the elderly. J. Neurosci. 28, 7031–7035. doi:10.1523/JNEUROSCI.0742-08.2008.

Brissenden, J.A., Tobyne, S.M., Osher, D.E., Levin, E.J., Halko, M.A., Somers Correspondence, D.C., 2018. Topographic cortico-cerebellar networks revealed by visual attention and working memory. Curr. Biol. 28, 3364–3372. doi:10.1016/j.cub.2018.08.059.

Burciu, R.G., Fritsche, N., Granert, O., Schmitz, L., Sponemann, N., Konczak, J., Theysohn, N., Gerwig, M., van Eimeren, T., Timmann, D., 2013. Brain changes associated with postural training in patients with cerebellar degeneration: a voxel-based morphometry study. J. Neurosci. 33, 4594–4604. doi:10.1523/JNEUROSCI.3381-12.2013.

Burman, D.D., 2019. Hippocampal connectivity with sensorimotor cortex during volitional finger movements: laterality and relationship to motor learning. PLoS One 14, e0222064. doi:10.1371/journal.pone.0222064.

Callaghan, M.F., Josephs, O., Herbst, M., Zaitsev, M., Todd, N., Weiskopf, N., 2015. An Evaluation of Prospective Motion Correction (PMC) for High Resolution Quantitative MRI. Frontiers in Neuroscience 9 9 (March), 97. doi:10.3389/fnins.2015.00097.

Campabadal, A., Segura, B., Junque, C., Iranzo, A., 2021. Structural and functional magnetic resonance imaging in isolated REM sleep behavior disorder: a systematic review of studies using neuroimaging software. Sleep Med. Rev. 59, 101495. doi:10.1016/j.smrv.2021.101495.

Canu, M.-H., Carnaud, M., Picquet, F., Goutebroze, L., 2009. Activity-dependent regulation of myelin maintenance in the adult rat. Brain Res. 1252, 45–51. doi:10.1016/j.brainres.2008.10.079.

Carlson, E.S., Stead, J.D.H., Neal, C.R., Petryk, A., Georgieff, M.K., 2007. Perinatal iron deficiency results in altered developmental expression of genes mediating energy metabolism and neuronal morphogenesis in hippocampus. Hippocampus 17, 679–691. doi:10.1002/HIPO.20307.

Clayden, J.D., Nagy, Z., Weiskopf, N., Alexander, D.C., Clark, C.A., 2015. Microstructural parameter estimation in vivo using diffusion MRI and structured prior information. Magn. Reson. Med. doi:10.1002/mrm.25723.

David, G., Mohammadi, S., Martin, A.R., Cohen-Adad, J., Weiskopf, N., Thompson, A., Freund, P., 2019. Traumatic and nontraumatic spinal cord injury: pathological insights from neuroimaging. Nat. Rev. Neurol. 1–14. doi:10.1038/s41582-019-0270-5.

Dayan, E., Cohen, L.G., 2011. Neuroplasticity subserving motor skill learning. Neuron 72, 443–454. doi:10.1016/j.neuron.2011.10.008.

Dick, F., Tierney, A.T., Lutti, A., Josephs, O., Sereno, M.I., Weiskopf, N., 2012. In vivo functional and myeloarchitectonic mapping of human primary auditory areas. J. Neurosci. 32, 16095–16105.

Dong, W.K., Greenough, W.T., 2004. Plasticity of nonneuronal brain tissue: roles in developmental disorders. Ment. Retard. Dev. Disabil. Res. Rev. 10, 85–90. doi:10.1002/mrdd.20016.

Doyon, J., Benali, H., 2005. Reorganization and plasticity in the adult brain during learning of motor skills. Curr. Opin. Neurobiol. 15, 161–167. doi:10.1016/j.conb.2005.03.004.

Draganski, B., Ashburner, J., Hutton, C., Kherif, F., Frackowiak, R.S.J., Helms, G., Weiskopf, N., 2011. NeuroImage regional specificity of MRI contrast parameter changes in normal ageing revealed by voxel-based quantification (VBQ). Neuroimage 55, 1423–1434. doi:10.1016/j.neuroimage.2011.01.052.

Draganski, B., Gaser, C., Kempermann, G., Kuhn, H.G., Winkler, J., Buchel, C., May, A., 2006. Temporal and spatial dynamics of brain structure changes during extensive learning. J. Neurosci. 26, 6314–6317. doi:10.1523/JNEUROSCI.4628-05.2006.

Draganski, B., May, A., 2008. Training-induced structural changes in the adult human brain. Behav. Brain Res. 192, 137–142. doi:10.1016/j.bbr.2008.02.015.

Edwards, L.J., Kirilina, E., Mohammadi, S., Weiskopf, N., 2018. Microstructural imaging of human neocortex in vivo. Neuroimage 182, 184–206. doi:10.1016/j.neuroimage.2018.02.055.

Eggenberger, P., Wolf, M., Schumann, M., de Bruin, E.D., 2016. Exergame and balance training modulate prefrontal brain activity during walking and enhance executive function in older adults. Front. Aging Neurosci. 8, 66. doi:10.3389/fnagi.2016.00066.

Eickhoff, S.B., Paus, T., Caspers, S., Grosbras, M.H., Evans, A.C., Zilles, K., Amunts, K., 2007. Assignment of functional activations to probabilistic cytoarchitectonic areas revisited. Neuroimage 36, 511–521. doi:10.1016/j.neuroimage.2007.03.060.

Eickhoff, S.B., Stephan, K.E., Mohlberg, H., Grefkes, C., Fink, G.R., Amunts, K., Zilles, K., 2005. A new SPM toolbox for combining probabilistic cytoarchitectonic maps and functional imaging data. Neuroimage 25, 1325–1335. doi:10.1016/j.neuroimage.2004.12.034.

Emmenegger, T.M., David, G., Ashtarayeh, M., Fritz, F.J., Ellerbrock, I., Helms, G., Balteau, E., Freund, P., Mohammadi, S., 2021. The influence of radio-frequency transmit field inhomogeneities on the accuracy of G-ratio weighted imaging. Front. Neurosci. 15, 1–17. doi:10.3389/fnins.2021.674719.

Erickson, K.I., Voss, M.W., Prakash, R.S., Basak, C., Szabo, A., Chaddock, L., Kim, J.S., Heo, S., Alves, H., White, S.M., Wojcicki, T.R., Mailey, E., Vieira, V.J., Martin, S.A., Pence, B.D., Woods, J.A., McAuley, E., Kramer, A.F., 2011. Exercise training increases size of hippocampus and improves memory. Proc. Natl. Acad. Sci. 108, 3017–3022. doi:10.1073/pnas.1015950108.

Fields, R.D., 2015. A new mechanism of nervous system plasticity: activity-dependent myelination. Nat. Rev. Neurosci. 16, 756–767. doi:10.1038/nrn4023.

Freund, P., Seif, M., Weiskopf, N., Friston, K., Fehlings, M.G., Thompson, A.J., Curt, A., 2019. MRI in traumatic spinal cord injury: from clinical assessment to neuroimaging biomarkers. Lancet Neurol. 18, 1123–1135. doi:10.1016/S1474-4422(19)30138-3.

Fu, M., Zuo, Y., 2011. Experience-dependent structural plasticity in the cortex. Trends Neurosci. 34, 177–187. doi:10.1016/j.tins.2011.02.001.

Georgiadis, M., Schroeter, A., Gao, Z., Guizar-Sicairos, M., Liebi, M., Leuze, C., McNab, J.A., Balolia, A., Veraart, J., Ades-Aron, B., Kim, S., Shepherd, T., Lee, C.H., Walczak, P., Chodankar, S., DiGiacomo, P., David, G., Augath, M., Zerbi, V., Sommer, S., Rajkovic, I., Weiss, T., Bunk, O., Yang, L., Zhang, J., Novikov, D.S., Zeineh, M., Fieremans, E., Rudin, M., 2021. Nanostructure-specific X-ray tomography reveals myelin levels, integrity and axon orientations in mouse and human nervous tissue. Nat. Commun. 12, 2941. doi:10.1038/s41467-021-22719-7.

Ghadery, C., Pirpamer, L., Hofer, E., Langkammer, C., Petrovic, K., Loitfelder, M., Schwingenschuh, P., Seiler, S., Duering, M., Jouvent, E., Schmidt, H., Fazekas, F., Mangin, J.-.F., Chabriat, H., Dichgans, M., Ropele, S., Schmidt, R., 2015. R2* mapping for brain iron: associations with cognition in normal aging. Neurobiol. Aging 36, 925–932. doi:10.1016/j.neurobiolaging.2014.09.013.

Gheysen, F., Van Opstal, F., Roggeman, C., Van Waelvelde, H., Fias, W., 2010. Hippocampal contribution to early and later stages of implicit motor sequence learning. Exp. Brain Res. 202, 795–807. doi:10.1007/s00221-010-2186-6.

Gibson, E.M., Purger, D., Mount, C.W., Goldstein, A.K., Lin, G.L., Wood, L.S., Inema, I., Miller, S.E., Bieri, G., Zuchero, J.B., Barres, B.A., Woo, P.J., Vogel, H., Monje, M., 2014. Neuronal activity promotes oligodendrogenesis and adaptive myelination in the mammalian brain. Science 344, 1252304. doi:10.1126/science.1252304.

Granert, O., Peller, M., Jabusch, H.-.C., Altenmüller, E., Siebner, H.R., 2011. Sensorimotor skills and focal dystonia are linked to putaminal grey-matter volume in pianists. J. Neurol. Neurosurg. Psychiatry 82, 1225–1231. doi:10.1136/jnnp.2011.245811.

Helms, G., Dathe, H., Kallenberg, K., Dechent, P., 2010. Erratum to: helms, dathe, kallenberg and dechent, high-resolution maps of magnetization transfer with inherent correction for rf inhomogeneity and T1 relaxation obtained from 3D FLASH MRI. Magn Reson Med 2008 Dec;60(6):1396-1407. Magn. Reson. Med. 64, 1856. doi:10.1002/mrm.22607.

Helms, G., Dathe, H., Kallenberg, K., Dechent, P., 2008. High-resolution maps of magnetization transfer with inherent correction for RF inhomogeneity and T 1 relaxation obtained from 3D FLASH MRI. Magn. Reson. Med. 60, 1396–1407. doi:10.1002/mrm.21732.

Helms, G., Dechent, P., 2009. Increased SNR and reduced distortions by averaging multiple gradient echo signals in 3D FLASH imaging of the human brain at 3T. J. Magn. Reson. 29, 198–204.

Hopkins, B.S., Weber, K.A., Cloney, M.B., Paliwal, M., Parrish, T.B., Smith, Z.A., 2018. Tract-specific volume loss on 3T MRI in patients with cervical spondylotic myelopathy. Spine 43, 1. doi:10.1097/BRS.0000000000002667.

Höysniemi, J., 2006. International survey on the dance dance revolution game. Comput. Entertain. 4. doi:10.1145/1129006.1129019.

Hüfner, K., Binetti, C., Hamilton, D.A., Stephan, T., Flanagin, V.L., Linn, J., Labudda, K., Markowitsch, H., Glasauer, S., Jahn, K., Strupp, M., Brandt, T., 2011. Structural and functional plasticity of the hippocampal formation in professional dancers and slackliners. Hippocampus 21, 855–865. doi:10.1002/hipo.20801.

Jackson, A.B., Dijkers, M., DeVivo, M.J., Poczatek, R.B., 2004. A demographic profile of new traumatic spinal cord injuries: change and stability over 30 years. Arch. Phys. Med. Rehabil. 85, 1740–1748. doi:10.1016/j.apmr.2004.04.035.

Jacobacci, F., Armony, J.L., Yeffal, A., Lerner, G., Amaro, E., Jovicich, J., Doyon, J., Della-Maggiore, V., 2020. Rapid hippocampal plasticity supports motor sequence learning. Proc. Natl. Acad. Sci. 117, 23898–23903. doi:10.1073/pnas.2009576117.

Kantor, D.B., Kolodkin, A.L., 2003. Curbing the excesses of youth. Neuron 38, 849–852. doi:10.1016/S0896-6273(03)00364-7.

Kearney, K.R., 2008. Instructional design and assessment a service-learning course for first-year pharmacy students. Am. J. Pharm. Educ. 72, 1–7.

Kempermann, G., Fabel, K., Ehninger, D., Babu, H., Leal-Galicia, P., Garthe, A., Wolf, S.A., 2010. Why and how physical activity promotes experience-induced brain plasticity. Front. Neurosci. 4, 189. doi:10.3389/fnins.2010.00189.

Kleim, J.A., Barbay, S., Cooper, N.R., Hogg, T.M., Reidel, C.N., Remple, M.S., Nudo, R.J., 2002. Motor learning-dependent synaptogenesis is localized to functionally reorganized motor cortex. Neurobiol. Learn. Mem. 77, 63–77. doi:10.1006/nlme.2000.4004.

Kodama, M., Ono, T., Yamashita, F., Ebata, H., Liu, M., Kasuga, S., Ushiba, J., 2018. Structural gray matter changes in the hippocampus and the primary motor cortex on an-hour-to-one- day scale can predict arm-reaching performance improvement. Front. Hum. Neurosci. 12, 209. doi:10.3389/fnhum.2018.00209.

Lakhani, B., Borich, M.R., Jackson, J.N., Wadden, K.P., Peters, S., Villamayor, A., MacKay, A.L., Vavasour, I.M., Rauscher, A., Boyd, L.A., 2016. Motor skill acquisition promotes human brain myelin plasticity. Neural Plast. 2016. doi:10.1155/2016/7526135.

Lamprecht, R., LeDoux, J., 2004. Structural plasticity and memory. Nat. Rev. Neurosci. 5, 45–54. doi:10.1038/nrn1301.

Langer, N., Hanggi, J., Muller, N.A., Simmen, H.P., Jancke, L., 2012. Effects of limb immobilization on brain plasticity. Neurology 78, 182–188.

Langkammer, C., Krebs, N., Goessler, W., Scheurer, E., Ebner, F., Yen, K., Fazekas, F., Ropele, S., 2010. Quantitative MR imaging of brain iron: a postmortem validation study. Radiology 257, 455–462. doi:10.1148/radiol.10100495.

Leutritz, T., Seif, M., Helms, G., Samson, R.S., Curt, A., Freund, P., Weiskopf, N., 2020. Multiparameter mapping of relaxation (R1, R2*), proton density and magnetization transfer saturation at 3 T: a multicenter dual-vendor reproducibility and repeatability study. Hum. Brain Mapp. 41, 4232–4247. doi:10.1002/hbm.25122.

Lissek, S., M, H., F, K., S, P., V, N., O, G., M, T., 2007. Sex differences in cortical and subcortical recruitment during simple and complex motor control: an fMRI study. Neuroimage 37. doi:10.1016/J.NEUROIMAGE.2007.05.037.

Long, J., Feng, Y., Liao, H., Zhou, Q., Urbin, M.A., 2018. Motor sequence learning is associated with hippocampal subfield volume in humans with medial temporal lobe epilepsy. Front. Hum. Neurosci. 12, 1–9. doi:10.3389/fnhum.2018.00367.

Lungu, O., Monchi, O., Albouy, G., Jubault, T., Ballarin, E., Burnod, Y., Doyon, J., 2014. Striatal and hippocampal involvement in motor sequence chunking depends on the learning strategy. PLoS One 9, e103885. doi:10.1371/journal.pone.0103885.

Maguire, E.A., Gadian, D.G., Johnsrude, I.S., Good, C.D., Ashburner, J., Frackowiak, R.S., Frith, C.D., 2000. Navigation-related structural change in the hippocampi of taxi drivers. Proc. Natl. Acad. Sci. U. S. A. 97, 4398–4403. doi:10.1073/pnas.070039597.

Makino, H., Hwang, E.J., Hedrick, N.G., Komiyama, T., 2016. Circuit mechanisms of sensorimotor learning. Neuron 92, 705–721. doi:10.1016/j.physbeh.2017.03.040.

Maller, J.J., Welton, T., Middione, M., Callaghan, F.M., Rosenfeld, J.V., Grieve, S.M., 2019. Revealing the hippocampal connectome through super-resolution 1150-direction diffusion MRI. Sci. Rep. 9, 1–13. doi:10.1038/s41598-018-37905-9.

McKenzie, I.A., Ohayon, D., Li, H., de Faria, J.P., Emery, B., Tohyama, K., Richardson, W.D., 2014. Motor skill learning requires active central myelination. Science 346, 318–322. doi:10.1126/science.1254960.Motor.

Middleton, F.A., Strick, P.L., 2000. Basal ganglia output and cognition: evidence from anatomical, behavioral, and clinical studies. Brain Cogn. 42, 183–200.

Möller, H.E., Bossoni, L., Connor, J.R., Crichton, R.R., Does, M.D., Ward, R.J., Zecca, L., Zucca, F.A., Ronen, I., 2019. Iron, myelin, and the brain: neuroimaging meets neurobiology. Trends Neurosci. 42, 384–401. doi:10.1016/j.tins.2019.03.009.

Moraud, E.M., Capogrosso, M., Formento, E., Wenger, N., DiGiovanna, J., Courtine, G., Micera, S., 2016. Mechanisms underlying the neuromodulation of spinal circuits for correcting gait and balance deficits after spinal cord injury. Neuron 89, 814–828. doi:10.1016/j.neuron.2016.01.009.

Natu, V.S., Gomez, J., Barnett, M., Jeska, B., Kirilina, E., Jaeger, C., Zhen, Z., Cox, S., Weiner, K.S., Weiskopf, N., Grill-Spector, K., 2019. Apparent thinning of human visual cortex during childhood is associated with myelination. Proc. Natl. Acad. Sci. U. S. A. 116, 20750–20759. doi:10.1073/pnas.1904931116.

Noah, J.A., Ono, Y., Nomoto, Y., Shimada, S., Tachibana, A., Zhang, X., Bronner, S., Hirsch, J., 2015. fMRI validation of fNIRS measurements during a naturalistic task. J. Vis. Exp. doi:10.3791/52116, e52116.

Orrell, A.J., Eves, F.F., Masters, R.S.W., 2006. Implicit motor learning of a balancing task. Gait Posture 23, 9–16. doi:10.1016/j.gaitpost.2004.11.010.

Park, I.S., Lee, K.J., Han, J.W., Lee, N.J., Lee, W.T., Park, K.A., Rhyu, I.J., 2009. Experience-dependent plasticity of cerebellar vermis in basketball players. Cerebellum 8, 334–339. doi:10.1007/s12311-009-0100-1.

Pereira, A.C., Huddleston, D.E., Brickman, A.M., Sosunov, A.A., Hen, R., McKhann, G.M., Sloan, R., Gage, F.H., Brown, T.R., Small, S.A., 2007. An in vivo correlate of exercise-induced neurogenesis in the adult dentate gyrus. Proc. Natl. Acad. Sci. 104, 5638–5643. doi:10.1073/pnas.0611721104.

Pinsard, B., Boutin, A., Gabitov, E., Lungu, O., Benali, H., Doyon, J., 2019. Consolidation alters motor sequence-specific distributed representations. Elife 8. doi:10.7554/eLife.39324.

Prahm, C., Kayali, F., Sturma, A., Aszmann, O., 2017. Recommendations For Games to Increase Patient Motivation During Upper Limb Amputee Rehabilitation. Springer, Cham, pp. 1157–1161. doi:10.1007/978-3-319-46669-9_188.

Purves, D., Augustine, G.J., Fitzpatrick, D., Hall, W.C., LaMantia, A.-.S., Mooney, R.D., Platt, M.L., White, L.E., 2018. Studying the nervous system. Neuroscience 1–29.

Rehfeld, K., Müller, P., Aye, N., Schmicker, M., Dordevic, M., Kaufmann, J., Hökelmann, A., Müller, N.G., 2017. Dancing or fitness sport? The effects of two training programs on hippocampal plasticity and balance abilities in healthy seniors. Front. Hum. Neurosci. 11, 305. doi:10.3389/fnhum.2017.00305.

Rhyu, I.J., Bytheway, J.A., Kohler, S.J., Lange, H., Lee, K.J., Boklewski, J., McCormick, K., Williams, N.I., Stanton, G.B., Greenough, W.T., Cameron, J.L., 2010. Effects of aerobic exercise training on cognitive function and cortical vascularity in monkeys. Neuroscience 167, 1239–1248. doi:10.1016/j.neuroscience.2010.03.003.

Ruegg, D.G., Kakebeeke, T.H., Gabriel, J.-.P., Bennefeld, M., 2003. Conduction velocity of nerve and muscle fiber action potentials after a space mission or a bed rest. Clin. Neurophysiol. 114, 86–93. doi:10.1016/S1388-2457(02)00329-2.

Sakayori, N., Kato, S., Sugawara, M., Setogawa, S., Fukushima, H., Ishikawa, R., Kida, S., Kobayashi, K., 2019. Motor skills mediated through cerebellothalamic tracts projecting to the central lateral nucleus. Mol. Brain 12, 13. doi:10.1186/s13041-019-0431-x.

Sampaio-Baptista, C., Johansen-Berg, H., 2017. White matter plasticity in the adult brain. Neuron 96, 1239–1251. doi:10.1016/j.neuron.2017.11.026.

Sampaio-Baptista, C., Khrapitchev, A.A., Foxley, S., Schlagheck, T., Scholz, J., Jbabdi, S., DeLuca, G.C., Miller, K.L., Taylor, A., Thomas, N., Kleim, J., Sibson, N.R., Bannerman, D., Johansen-Berg, H., 2013. Motor skill learning induces changes in

white matter microstructure and myelination. J. Neurosci. 33, 19499–19503. doi:10.1523/JNEUROSCI.3048-13.2013.

Sampaio-Baptista, C., Vallès, A., Khrapitchev, A.A., Akkermans, G., Winkler, A.M., Foxley, S., Sibson, N.R., Roberts, M., Miller, K., Diamond, M.E., Martens, G.J.M., De Weerd, P., Johansen-Berg, H., 2020. White matter structure and myelin-related gene expression alterations with experience in adult rats. Prog. Neurobiol. 187. doi:10.1016/j.pneurobio.2020.101770.

Schlegel, A.A., Rudelson, J.J., Tse, P.U., 2012. White matter structure changes as adults learn a second language. J. Cogn. Neurosci. 24, 1664–1670. doi:10.1162/jocn_a_00240.

Schmierer, K., Scaravilli, F., Altmann, D.R., Barker, G.J., Miller, D.H., 2004. Magnetization transfer ratio and myelin in postmortem multiple sclerosis brain. Ann. Neurol. 56, 407–415. doi:10.1002/ana.20202.

Schneider, R., Gautier, J.-.C., Gautier, Jean-Claude, 1994. Site of lesions, weakness patterns and causes. Brain.

Scholz, J., Klein, M.C., Behrens, T.E.J., Johansen-Berg, H., 2009. Training induces changes in white-matter architecture. Nat. Neurosci. 12, 1370–1371. doi:10.1038/nn.2412.

Sehm, B., Taubert, M., Conde, V., Weise, D., Classen, J., Dukart, J., Draganski, B., Villringer, A., Ragert, P., 2014. Structural brain plasticity in Parkinson's disease induced by balance training. Neurobiol. Aging 35, 232–239. doi:10.1016/j.neurobiolaging.2013.06.021.

Sommer, M.A., 2003. The role of the thalamus in motor control this review comes from a themed issue on motor systems edited by John P Donoghue and Okihide Hikosaka. Curr. Opin. Neurobiol. 13, 663–670. doi:10.1016/j.conb.2003.10.014.

Streitbürger, D.-.P., Möller, H.E., Tittgemeyer, M., Hund-Georgiadis, M., Schroeter, M.L., Mueller, K., 2012. Investigating structural brain changes of dehydration using voxel-based morphometry. PLoS One 7, e44195. doi:10.1371/journal.pone.0044195.

Tabelow, K., Balteau, E., Ashburner, J., Callaghan, M.F., Draganski, B., Helms, G., Kherif, F., Leutritz, T., Lutti, A., Phillips, C., Reimer, E., Ruthotto, L., Seif, M., Weiskopf, N., Ziegler, G., Mohammadi, S., 2019. Hmri—a toolbox for quantitative MRI in neuroscience and clinical research. Neuroimage 194, 191–210. doi:10.1016/j.neuroimage.2019.01.029.

Taubert, M., Mehnert, J., Pleger, B., Villringer, A., 2016. Rapid and specific gray matter changes in M1 induced by balance training. Neuroimage 133, 399–407. doi:10.1016/j.neuroimage.2016.03.017.

Theodosis, D.T., Poulain, D.A., Oliet, S.H.R.R., 2008. Activity-dependent structural and functional plasticity of astrocyte-neuron interactions. Physiol. Rev. 88, 983–1008. doi:10.1152/physrev.00036.2007.

Thomas, A.G., Dennis, A., Rawlings, N.B., Stagg, C.J., Matthews, L., Morris, M., Kolind, S.H., Foxley, S., Jenkinson, M., Nichols, T.E., Dawes, H., Bandettini, P.A., Johansen-Berg, H., 2016. Multi-modal characterization of rapid anterior hippocampal volume increase associated with aerobic exercise. Neuroimage 131, 162–170. doi:10.1016/j.neuroimage.2015.10.090.

Toscano-Silva, M., da Silva, S.G., Scorza, F.A., Bonvent, J.J., Cavalheiro, E.A., Arida, R.M., 2010. Hippocampal mossy fiber sprouting induced by forced and voluntary physical exercise. Physiol. Behav. 101, 302–308. doi:10.1016/j.physbeh.2010.05.012.

Tran, P.V., Kennedy, B.C., Lien, Y.C., Simmons, R.A., Georgieff, M.K., 2015. Fetal iron deficiency induces chromatin remodeling at the Bdnf locus in adult rat hippocampus. Am. J. Physiol. Regul. Integr. Comp. Physiol. 308, R276–R282. doi:10.1152/AJPREGU.00429.2014.

Tronel, S., Fabre, A., Charrier, V., Oliet, S.H.R., Gage, F.H., Abrous, D.N., 2010. Spatial learning sculpts the dendritic arbor of adult-born hippocampal neurons. Proc. Natl. Acad. Sci. U. S. A. 107, 7963–7968. doi:10.1073/pnas.0914613107.

Villiger, M., Grabher, P., Hepp-Reymond, M.-.C., Kiper, D., Curt, A., Bolliger, M., Hotz-Boendermaker, S., Kollias, S., Eng, K., Freund, P., 2015. Relationship between structural brainstem and brain plasticity and lower-limb training in spinal cord injury: a longitudinal pilot study. Front. Hum. Neurosci. 9, 1–10. doi:10.3389/fnhum.2015.00254.

Watson, T.C., Obiang, P., Torres-Herraez, A., Watilliaux, A., Coulon, P., Rochefort, C., Rondi-Reig, L., 2019. Anatomical and physiological foundations of cerebello-hippocampal interaction. Elife 8. doi:10.7554/eLife.41896.

Weber, B., Koschutnig, K., Schwerdtfeger, A., Rominger, C., Papousek, I., Weiss, E.M., Tilp, M., Fink, A., 2019. Learning unicycling evokes manifold changes in gray and white matter networks related to motor and cognitive functions. Sci. Rep. 9, 4324. doi:10.1038/s41598-019-40533-6.

Weiskopf, N., Edwards, L.J., Helms, G., Mohammadi, S., Kirilina, E., 2021. Quantitative magnetic resonance imaging of brain anatomy and in vivo histology. Nat. Rev. Phys. 3, 570–588. doi:10.1038/s42254-021-00326-1.

Weiskopf, N., Lutti, A., Helms, G., Novak, M., Ashburner, J., Hutton, C., 2011. Unified segmentation based correction of R1 brain maps for RF transmit fi eld inhomogeneities (UNICORT). Neuroimage 54, 2116–2124. doi:10.1016/j.neuroimage.2010.10.023.

Weiskopf, N., Suckling, J., Williams, G., Correia, M.M., Inkster, B., Tait, R., Ooi, C., Bullmore, E.T., Lutti, A., 2013. Quantitative multi-parameter mapping of R1, PD(*), MT, and R2(*) at 3T: a multi-center validation. Front. Neurosci. 7, 1–11. doi:10.3389/fnins.2013.00095.

Wenger, E., Kühn, S., Verrel, J., Mårtensson, J., Bodammer, N.C., Lindenberger, U., Lövdén, M., 2016. Repeated structural imaging reveals nonlinear progression of experience-dependent volume changes in human motor cortex. Cereb. Cortex bhw141. doi:10.1093/cercor/bhw141.

Yang, G., Pan, F., Gan, W.-.B., 2009. Stably maintained dendritic spines are associated with lifelong memories. Nature 462, 920–924. doi:10.1038/nature08577.

Yasuda, M., Johnson-Venkatesh, E.M., Zhang, H., Parent, J.M., Sutton, M.A., Umemori, H., 2011. Multiple forms of activity-dependent competition refine hippocampal circuits in vivo. Neuron 70, 1128–1142. doi:10.1016/j.neuron.2011.04.027.

Yeung, M.S.Y., Zdunek, S., Bergmann, O., Bernard, S., Salehpour, M., Alkass, K., Perl, S., Tisdale, J., Possnert, G., Brundin, L., Druid, H., Frisén, J., 2014. Dynamics of oligodendrocyte generation and myelination in the human brain. Cell 159, 766–774. doi:10.1016/j.cell.2014.10.011.

Zatorre, R.J., Fields, R.D., Johansen-Berg, H., 2012. Plasticity in gray and white: neuroimaging changes in brain structure during learning. Nat. Neurosci. 15, 528–536. doi:10.1038/nn.3045.

Ziegler, G., Grabher, P., Thompson, A., Altmann, D., Hupp, M., Ashburner, J., Friston, K., Weiskopf, N., Curt, A., Freund, P., 2018. Progressive neurodegeneration following spinal cord injury: implications for clinical trials. Neurology 90 (14), e1257–e1266. doi:10.1212/WNL.0000000000005258.